Diffusing fraction of niche BMP ligand safeguards stem-cell differentiation

Sharif M. Ridwan[1], Autumn Twillie[1], Shinya Matsuda[2], Matthew Antel[1], Muhammed Burak Bener[1] Ann E. Cowan[3, 4] and Mayu Inaba[1,*]

1. Department of Cell Biology, University of Connecticut Health Center, Farmington, Connecticut, United States of America
2. Biozentrum, University of Basel, Basel, Switzerland
3. Richard D. Berlin Center for Cell Analysis and Modeling, University of Connecticut Health Center, Farmington, Connecticut, United States of America,
4. Department of Molecular Biology and Biophysics, University of Connecticut Health Center, Farmington, Connecticut, United States of America

[*] Correspondence: inaba@uchc.edu

One sentence summary: A soluble BMP ligand diffuses from the niche and has dual, and opposite roles on stem cells and differentiating daughter cells.

Abstract

Drosophila male germline stem cells (GSCs) reside at the tip of the testis and surround a cluster of niche cells. It has been believed that the niche-derived Decapentaplegic (Dpp) ligand has a role in maintaining stem cells in close proximity but has no role in the differentiating cells spaced one-cell layer away. However, the range of Dpp diffusion has never been tested. Here, using genetically encoded nanobodies called Morphotrap, we physically block Dpp diffusion without interfering with niche-stem cell signaling. When Dpp diffusion is perturbed, differentiating germ cells frequently de-differentiated, suggesting that Dpp ensures differentiation of GSC daughter cells, opposing to its role in maintenance of GSC in the niche. Our work provides the evidence that a single niche ligand induces distinct cellular responses inside versus outside the niche, which may be a common mechanism to regulate tissue homeostasis.

Introduction

The stem cell niche was initially proposed to be a limited space in tissues or organs where tissue stem cells reside. Based on the phenomenon in which transplantation of hematopoietic stem cells is only successful when naïve stem cells are depleted, a niche is thought to provide a suitable environment for stem cells to self-renew(*1*, *2*). At the same time, the niche environment should not foster the differentiation of descendant cells in order to ensure that the correct balance of self-renewal and differentiation is maintained(*2-4*). Although 40 years have passed since this niche concept was originally proposed(*1*), the mechanism of niche signal restriction is still largely unknown(*5*). This is partly because of the difficulty in studying stem cells in their *in vivo* context. Moreover, the dispersion of broad signaling molecules secreted from the niche is notoriously difficult to assess.

The *Drosophila* germline stem cell system provides a model to study niche-stem cell interaction. The niche, called the hub, is composed of post-mitotic hub cells. Each testis contains a single hub harboring 8-14 germline stem cells (GSCs) which directly attach to the hub(*6*). The division of a GSC is almost always asymmetric via formation of stereotypically oriented spindle, producing a new GSC and a gonialblast (GB), the differentiating daughter cell(*7*). After being displaced away from the hub, the GB enters 4 rounds of transit-amplifying divisions to form 2 to 16 cell spermatogonia (SGs). Then, 16-cell SGs become spermatocytes (SCs) and proceed to meiosis (Figure 1A-B)(*8*).

The Bone Morphogenetic Protein (BMP) ligand is often utilized in many stem cell niches in diverse systems(*9*). In the *Drosophila* testis, the BMP ligand, Decapentapledic (Dpp) has emerged as major ligand in the GSC niche together with a cytokine-like ligand, Unpaird (Upd)(*10-14*). In the testis, it has been hypothesized that these signals are only activated within GSCs in close contact to the hub, and immediately downregulated in GBs that are detached from the hub. However, the range of diffusion of these ligands and whether ligand diffusion beyond the niche space has a role is unknown.

We previously demonstrated that hub-derived Dpp ligand is received by GSC-specific membrane protrusions, which we termed microtubule based (MT) -nanotubes, to efficiently activate downstream pathways within the GSC population(*15*). MT-nanotubes likely provide sufficient surface area along their length to allow the plasma membranes of GSCs and hub cells to closely contact one another for signaling(*15, 16*). This suggested the possibility that the Dpp signal is transmitted in a contact-dependent manner.

Furthermore, we serendipitously found that Dpp ligand from the hub is able to diffuse farther from the niche than previously thought(*17*), suggesting that Dpp ligand secreted from the niche could provide both contact-dependent and contact-independent signals. Besides the apparent contact-dependent signaling role of Dpp in the niche, we wondered what role the diffusing fraction of Dpp ligand plays in the cells located outside of the niche.

In this study, we now directly address the function of the diffusing fraction of Dpp outside of the niche. We apply a previously established tool, Morphotrap, a genetically encoded nanobody that can trap secretory ligands on the plasma membrane of ligand-secreting cells(*18, 19*). Unexpectedly, we found that Dpp has distinct roles in GSCs as compared to differentiating germ cells, such as promoting self-renewal of GSCs and blocking de-differentiation of GBs and SGs.

Results

Dpp diffuses from niche to the anterior area of the testis

We previously showed that overexpressed Dpp ligand from the hub can diffuse outside of the niche(*17*). However, we were not able to successfully visualize a diffusing fraction of Dpp at endogenous protein levels to show that this behavior is physiological. For this study, we tackled this challenge by generating a fly line that expresses mGreen Lantern-tagged Dpp (*mGL-dpp*) from the endogenous locus, as described previously(*20*), so that we can monitor endogenous Dpp behavior (Figure 1C). Because the homozygous expression of *mGL-dpp* is semilethal, we introduced a wild-type *dpp* transgene expressed only in embryonic stage(*21*). These rescued *mGL-dpp* flies were fully viable and able to reach adulthood with no phenotypes observed in the testis. Using these flies allowed us to successfully visualize endogenous Dpp expression and localization in the testis, as mGL-Dpp signal was seen throughout the tissue at levels above the background fluorescence (Figure 1D-E).

We noticed that mGL-Dpp localized in a pattern reminiscent of the extracellular space between cells throughout the testis, and was not restricted to the niche (Figure 1E). Next we incubated testes in the media with freely diffusible fluorescent 10KDa dextran dye, that is similar size of Dpp protein (14.8KDa), in a short period of time (~5 min). Fluorescence was observed throughout the tissue in extracellular spaces between SG cysts and between germline and

surrounding cyst cells as previously described (Figure 1F)(*22*), in a pattern that similar to mGL-Dpp distribution, appeared to surround interconnected germ cells at various stages of SG differentiation (Figure 1G-I). This suggested that mGL-Dpp localizes to extracellular space between the germline and the soma (Figure 1J).

As the localization pattern of the diffusible dextran dye and mGL-Dpp were similar, we hypothesized that the mGL-Dpp signal resulted from diffusion of the molecule throughout the tissue. To assess the mobility of fraction of mGL-Dpp in the tissue, we performed a fluorescence recovery after photobleaching (FRAP) analysis. After photobleaching, an average of ~20% of mGL-Dpp signal quickly recovered within a few minutes (Figure 1K-K'), suggesting that there may be two distinct fractions of the molecule present in the tissue: a mobile fraction (20% of total) that is freely diffusing, likely from the niche, and an immobile fraction (80% of the total) that is likely trapped in extracellular spaces or internalized by cells.

Taken together, these data indicate that endogenous Dpp is freely diffusible throughout the extracellular space of the testis.

Perturbation of Dpp diffusion without affecting niche-GSC signal

While Dpp function within the niche is well-characterized, the role of a potentially diffusible Dpp fraction outside of the niche is completely unknown. In order to assess the function of the diffusing fraction of Dpp, we sought to specifically disturb only this diffusing population, without affecting the immobile niche-GSC Dpp signal. To achieve this, we utilized the morphotrap (MT), a genetically encoded tool consisting of a fusion protein between a transmembrane protein and a nanobody that acts as a synthetic receptor for tagged proteins(*18*, *19*). We used two versions of MT, each expressing a fusion protein of a nanobody that recognizes Green fluorescent protein (GFP) (and its variants, including mGL) and one of two different transmembrane proteins, Nrv1 or mCD8 (Figure 2A). Nrv-MT consists of the Nrv1 protein scaffold and localizes to the basolateral compartment of the *Drosophila* wing disc(*19*). mCD8-MT consists of the membrane protein mCD8 and localizes throughout the entire plasma membrane(*19*). In order to trap Dpp diffusing from the niche (hub) with MT, we utilized the hub driver fasIIIGal4, which drives expression specifically in the hub cells that make up the germline stem cell niche (Figure 2B, C). By expressing MT under control of the fasIIIGal4 driver in the

mGL-dpp homozygous background, we reasoned that we could effectively trap mGL-Dpp on hub cell membranes and thus prevent its diffusion (Figure 2B).

Indeed, we found that expression of both Nrv-MT and mCD8-MT under the fasIIIGal4 driver eliminated mGL-Dpp signal throughout the testis (Figure 2D-F), indicating that both Morphotraps can efficiently trap mGL-tagged Dpp. In both conditions, trapping Dpp did not perturb pMad signal in somatic cyst cells (Figure S1A, B), which suggests that pMad in cyst cells is not activated by hub-derived diffusing Dpp and serves as a reliable internal control for quantifying relative pMad intensity in germ cells.

We observed slightly different pattern of trapped mGL-Dpp signal in the hub between the two MTs: although Nrv-MT often showed colocalization of mGL-Dpp signal with FM4-64 membrane dye, mCD8-MT tended to show mGL-Dpp signal separated from the membrane and cytoplasm of hub cells (Figure S2A, B), indicating that mGL-Dpp trapped by mCD8-MT could be internalized into hub cells. Therefore, we were concerned that that Dpp signaling between hub and GSC may be affected by mGL-Dpp, fasIII>mCD8-MT. To test this, we stained for phosphorylated Mad (mothers against dpp) protein, a readout of Dpp signal activation. Phosphorylated Mad (pMad) was reduced in GSCs in mGL-Dpp, fasIII>mCD8-MT testes (Figure 2G-J), likely because of internalization of trapped Dpp (Figure S2B). In comparison, mGL-Dpp, fasIII>Nrv-MT showed similar pMad intensities in the GSCs as compared to control sample (Figure 2G-J), indicating that Dpp signaling between the hub and the GSCs was unaffected. Based on these results, we concluded that fasIII>Nrv-MT expression in the *mGL-dpp* homozygous background was the best tool to be used to assess the function(s) of hub-derived Dpp outside of the niche, without disrupting hub-GSC Dpp signaling.

Expression of Nrv-MT using the germline driver nosGal4 (mGL-Dpp, nos>Nrv-MT) resulted in mGL-Dpp trapping along the membranes of germ cells outside of the niche (Figure 2K, L) and hyper-activation of signaling outside of the niche, as indicated by elevated pMad staining (Figure 2M, N). These data further confirm that a fraction of Dpp is diffusible and trappable by the MT method, and that trapped Dpp can still signal to receptors present on the plasma membrane of the cells.

The diffusing fraction of Dpp prevents de-differentiation outside the niche

In the *Drosophila* testis, GSCs almost exclusively divide asymmetrically to produce one GSC and one GB (asymmetric outcome, Figure 3A)(*7, 23, 24*). However, symmetric GSC division can also occur (symmetric outcome, Figure 3A)(*23, 24*). These symmetric events occur via two mechanisms: 1) spindle misorientation, where the mitotic spindle orients parallel to the hub-GSC interface, resulting in two GSCs (Figure 3A-□)(*7*), and 2) de-differentiation, where a differentiating GB or SG physically relocates back to the niche and reverts to a GSC identity (Figure 3A-□)(*25*). The de-differentiation has been shown to be required for replenishing lost stem cells to maintain stem cell number(*26*). At the same time, excessive de-differentiation can be a cause of tumorigenesis(*27*).

By scoring the orientation of cells still interconnected by the fusome, a germline-specific organelle that branches throughout germ cells during division, we can estimate the frequency of symmetric events in the niche(*24, 25, 28*). We noticed that mGL-Dpp, fasIII>Nrv-MT testes showed a significantly higher frequency of symmetric events than the control (Figure 3B-D), suggesting that preventing Dpp diffusion results in more GSC symmetric outcomes.

It has been hypothesized that de-differentiation is required for GSC maintenance during fly age(*28*). In mGL-Dpp, fasIII>Nrv-MT testes, the number of GSCs at the hub were slightly higher at timepoints of day 14 and 21 post-eclosion (Figure 3E), suggesting the possibility that preventing Dpp diffusion may cause excess de-differentiation.

In the *Drosophila* testis, Bag of marbles (Bam), a translational repressor that is expressed after a germ cell exits the GSC state and is sufficient for promoting differentiation(*25*). Using heat-shock inducible expression of Bam in GSCs, we can artificially induce differentiation of GSCs, resulting in depletion of all GSCs from the niche. After the flies are recovered in normal temperature, the niche is replenished by de-differentiation(*25*). By introducing *hs-bam* transgene in the *mGL-dpp* homozygous background with or without fasIII>Nrv-MT expression, we assessed the function of the diffusible Dpp fraction on de-differentiation. Strikingly, induction of GSC differentiation in mGL-Dpp, fasIII>Nrv-MT flies resulted in a significantly faster recovery of GSCs in the niche as compared to flies without fasIII>Nrv-MT expression (Figure3F, H). Moreover, Dpp trapping using an alternative driver/knock-in combination (dppGal4>Nrv-MT, *GFP-dpp* knock-in homozygous background) showed similar effect on de-differentiation (Figure S3), confirming that the trapping Dpp is the cause of observed phenotype.

These data suggests that diffusible Dpp plays a role in preventing de-differentiation in differentiating GBs and SGs. Since the Nrv-MT only affect differentiating cells located away from the niche, but not GSCs within the niche, we speculated that increased de-differentiation rather than increased spindle misorientation may be responsible for observed high frequency of symmetric events. To further rule out the possibility that the effects are instead caused by defects in spindle orientation in the GSCs that result in symmetric division, we assessed the spindle orientations of GSCs in the mGL-Dpp, fasIII>Nrv-MT flies. We found that GSCs showed correctly oriented spindles (Figure 3I-M), in support of our conclusions that that observed symmetric outcome are the result of excess de-differentiation and not spindle misorientation. We do observe that although the spindles were correctly oriented, centrosomes of GSCs in mGL-Dpp, fasIII>Nrv-MT flies were significantly more misoriented (Figure 3I-M), but this is likely a secondary effect of a higher frequency of de-differentiation as de-differentiated GSCs are reported to have higher instances of centrosome misorientation(*29*).

Dpp acts through its canonical pathway in GSCs and in differentiating germ cells

We next asked if Dpp acts within the same signaling pathway in differentiating germ cells as it does in GSCs. Dpp is known to bind to its receptor Thickveins (Tkv) on GSCs and activate Tkv-mediated signaling to maintain GSC identity(*10, 11*). Knock-down of Tkv by expression of shRNA under the control of the germline driver nosGal4 results in a depletion of GSCs from the niche (Figure 4A-B), demonstrating the indispensability of this pathway to GSC maintenance consistent with previous reports(*10, 11*).

To determine if Tkv is the receptor for diffusible Dpp for germ cells outside of the niche, we knocked down Tkv exclusively in differentiating germ cells using the driver bamGal4. Intriguingly, we observed a higher number of GSCs per niche in bam>Tkv RNAi testes as flies aged (Figure 4C), similar to what was observed in mGL-Dpp, fasIII>Nrv-MT flies (Figure 3E). Moreover, bam>Tkv RNAi testes also exhibit a higher frequency of symmetric events (Figure 4D-F), recapitulating the phenotype of mGL-Dpp, fasIII>Nrv-MT flies and suggesting that Tkv-mediated signaling in differentiating germ cells may similarly result in higher instances of de-differentiation. Indeed, analysis of hs-bam with bam>Tkv RNAi show a significantly faster recovery of GSCs than control after heat-shock mediated depletion of GSCs (Figure 4G), indicating Tkv-mediated signaling in differentiating cells impedes de-differentiation. Next, we

knocked-down Mad, the downstream effector of Tkv-signaling, and Medea, the partner of Mad, using bamGal4 mediated shRNA expression in hs-bam flies. We found that both RNAi conditions show a significantly faster recovery of GSCs after heat-shock mediated GSC depletion, indicating the Tkv-Mad/Medea pathway that is responsible for maintenance of GSCs, is also responsible for preventing de-differentiation.

As was the case of mGL-Dpp, fasIII>Nrv-MT flies, spindles were not misoriented in all *bam>tkv RNAi*, *bam>mad RNAi* and *medea RNAi* genotypes (Figure S4A), again suggesting that de-differentiation, and not spindle misorientation, is responsible for the increase in symmetric events. Centrosomes for these genotypes did exhibit misorientation but noted above, this is a phenomenon frequently seen in GSCs as a consequence of de-differentiation.

These data suggest that both the mobile and diffusing fraction of Dpp (inside and outside of the niche) can signal through same signaling pathway that activates Mad.

Dpp signal oppositely regulates Bam expression in GSCs and in differentiating germ cells

It has been known that Dpp signal suppress expression of bam gene in GSCs(*11*). Bam is necessary and sufficient for differentiation and its suppression in stem cells is essential to maintain their undifferentiated states(*11*). Therefore, we next wondered whether Dpp signal oppositely acts on Bam between GSCs and differentiating cells. To test this possibility, we examined Bam expression level in the testes in which Dpp diffusion is blocked by Morphotrap (mGL-Dpp, fasIII>Nrv-MT).

If Dpp signal acts on Bam in differentiating cells to inhibit dedifferentiation, Dpp needs to enhance Bam expression, thus blocking Dpp diffusion would reduce Bam expression in differentiating cells. To test this, we blocked Dpp diffusion using Morphotrap and stained these testes with Bam. As we expected, Bam expression was reduced in Morphotrap genotypes (Figure 5A-D). Similar Bam reduction was also observed in bam>Tkv RNAi and bam>Mad RNAi testes (Figure 5E-H), suggesting that Mad upregulates Bam expression in these differentiating cell populations located outside of the niche, opposed to its repressor function in GSCs.

To test whether reduced Bam levels is functionally responsible for accelerating de-differentiation, we attempted to rescue the bam>Tkv RNAi phenotype by combining it with Bam overexpression. Strikingly, bamGal4 mediated expression of Bam almost completely abrogated the observed enhancement of de-differentiation in bam>Tkv RNAi alone (Figure 5I), indicating

that Dpp signal outside of the hub inhibits de-differentiation through augmentation of Bam expression.

Mad switches its function on *bam* promoter in a concentration dependent manner

So far, our data suggest that Dpp-Tkv-Mad axis downregulates Bam expression in GSCs, while it upregulates Bam expression in GB/SGs. How does the same pathway oppositely regulate same target gene *bam*? It has been shown that concentration of Dpp linearly correlates to pMad concentration in the morphogen fields(*30*). In the testis, Dpp signal is highest in GSCs seen as strong pMad intensity and it immediately becomes lower in GB/SGs (Figure 2G). Therefore, we wondered if the opposed Dpp function depends on the pMad concentration. To test this possibility, we attempted to ectopically hyperactivate signal by trapping Dpp on the membrane of germ cells. Expression of Nrv-MT using the germline driver nosGal4 (mGL-Dpp, nos>Nrv-MT) results in high pMad accumulation in the cells outside of the niche (Figure 2N). We stained Bam in this genotype and found that SGs strongly trapping Dpp are often negative with Bam staining, while SGs weakly trapping Dpp show high intensity of Bam (Figure 6A), suggesting that function of Dpp on Bam expression is likely concentration dependent. Moreover, we found that germline tumors induced by overexpression of constitutive active form of Tkv (nos>TkvCA) are mixture of Bam positive and negative cells (Figure 6B), supporting our hypothesis that Dpp signal has dual role on *bam* expression. To further confirm opposite outcome of Dpp signal inside and outside the niche is dependent on Mad concentration, we next compared effect of bam>Mad RNAi and bam>Mad overexpression on de-differentiation. Strikingly, overexpression of Mad (bam>Mad) in hs-Bam flies show a significant reduction of recovery rate of GSCs after heat-shock mediated GSC depletion (Figure 6C), opposed to the effect of bam>Mad RNAi, suggesting that Mad switches its function from repressor to activator in a concentration dependent manner.

The Mad binding domain in the *bam* promoter has been well-characterized in female GSCs(*31*, *32*). In addition to previously characterized Mad binding site (position +39 from the transcription start site) required for silencing *bam* in female GSCs, *bam* promoter possesses another putative Mad binding site at position -68 (Figure 6D)(*31*, *32*). We speculated that different Mad occupancy on these two cites may be involved in different outcome. To examine requirement of these two cites in GSC and differentiating cells, we generated transgenic flies

harboring bam promoter reporter constructs with or without mutations on these two Mad binding sites. Unexpectedly, we found that +39 and -68 sites are both required to suppress Bam expression in GSCs, as both mutations cause precocious expression of *bam* reporter in GSCs (Figure 6E-G lower panels), suggesting that high concentration of pMad may allow them to occupy both sites, which may be required for repressor function. Furthermore, we noticed that +39 mutated- but not -68 mutated-reporter shows drastically lower intensity than control reporter in 4-8 SGs (Figure 6E-H), indicating that the +39 site is required for upregulation of Bam in differentiating cells. This result suggests that Dpp signaling from a diffusing fraction of Dpp upregulates *bam* expression through +39 Mad binding site in *bam* promoter to activate its transcription to ensure differentiation of cells (Figure 6I). It should be noted that the -68 mutated Bam reporter did not show the signal in GSCs as high as 2-4 SGs (Figure 6F), indicating that removing pMad from -68 site is necessary but not sufficient to fully activate bam promoter, suggesting the existence of other co-activator in 2-4 SGs (Figure 6I).

Taken together, this study provides clear evidence that a soluble niche ligand can diffuse from a niche and form a gradient. And it facilitates differential signaling responses in stem cells and their differentiating progenies, proving a new paradigm of niche space restriction (Figure 6J).

Discussion

In this study, we demonstrated that the niche BMP ligand, Dpp, has function beyond contact-dependent signals in the stem cell niche. We showed that diffusible Dpp has a key function outside the niche in promoting GSC daughter cells to differentiate, a role opposite to its function in the niche in promoting the self-renewal of GSCs. These distinct signaling outcomes are achieved by the same canonical BMP pathway, via receptor Tkv and downstream effector Mad, which then represses Bam expression in stem cells but upregulates Bam expression in differentiating cells.

Signaling from the stem cell niche is believed to maintain the “stemness” of resident stem cells and the niche Dpp signal has been postulated to act as a highly localized niche signal. Using *Drosophila* male and female gonads, many studies have revealed how a steep gradient of BMP response is established within just one cell diameter that maintains a GSC fate(*33-44*). Many of these studies postulated redundant mechanisms in which differentiating cells actively suppress downstream molecules, leaving the possibility that the diffusion of Dpp may be present(*45*).

However, no study has specifically assessed the function of diffusing fraction of Dpp. In this study we provide the evidence that niche-derived Dpp can diffuse beyond 1-cell diameter and facilitate different signaling responses in differentiating progenies as compared to stem cells. Such behavior of Dpp is reminiscent to its function in morphogen field where Dpp creates gradient over a long distance and induces pMad accumulation on target gene promoters in a graded manner during early embryonic development(*46*).

The mechanism by which Mad function switches between downregulation and upregulation of Bam expression remains elusive. A study demonstrated that the Dpp gradient linearly correlates to pMad gradient in the tissue(*30*), and pMad interact with different co-factors in a concentration-dependent manner and act as either a transcriptional repressor or activator(*47*). Further molecular studies will require to fully understand this phenomenon in stem-cell system.

Since mammalian homologs of Dpp, the TGF-beta family genes, are broadly utilized in many stem cell niches(*9*), we propose that diffusion of the ligands might be a common mechanism in stem cell niches to ensure their spatial restriction and asymmetric outcome of stem cell division. Intriguingly, differential effects of a BMP ligand, transforming growth factor (TGF)-β, albeit focused on proliferation, has been reported in hematopoietic stem cell (HSC) niche, where low concentrations of TGF-β induces proliferation of myeloid-biased HSCs but inhibit proliferation of lymphoid-biased HSCs (Ly-HSCs)(*48*, *49*). In this case, it is still unknown whether the ligand forms a gradient around HSC niche and whether these progenitors are located distinct positions that subject them to different TGF-β concentrations. The elucidation of the basis of these differential outputs based on ligand behavior is a fascinating topic for future study.

Acknowledgements

We thank Markus Affolter for discussion and suggestions. Thomas Kornberg, Yukiko Yamashita, Michael Buszczak, Cheng-Yu-Lee and the Bloomington Drosophila Stock Center and the Developmental Studies Hybridoma Bank for reagents; Marie Bao (Life Science Editors) for manuscript editing. This research is supported by R35GM128678 from the National Institute for General Medical Sciences and a start-up fund from UConn Health (to M.I.) and an SNSF Ambizione grant (PZ00P3_180019) (to S.M.).

Author Contributions

M.I., S.M.R., conceived the project. M.I., S.M.R., A.T. and M.A., designed and executed experiments and analyzed data. S.M. generated *mGL-dpp* line and assisted with the design of the experiments. M.B.B. generated *UASp-bam* transgenic fly. A.E.C., quantitative analysis and interpretation of imaging data. S.M.R., M.I., drafted manuscript. All authors edited the manuscript.

Declaration of Interests

The authors declare no competing interests.

Materials and Methods

Fly husbandry and strains

Flies were raised on standard Bloomington medium at 25°C (unless temperature control was required). The following fly stocks were obtained from Bloomington stock center (BDSC); *nosGal4* (BDSC64277); *hs-bam* (BDSC24636); *tkv RNAi* (BDSC40937); Nrv1 morphotrap (*lexAop-UAS-GrabFP.B.Ext.TagBFP*, BDSC68173); mCD8-morphotrap *(lexAop-UAS-morphotrap.ext.mCh*, BDSC68170); *medea RNAi:TRiP.GL01313* (BDSC43961); *mad RNAi:TRiP.JF01264* (BDSC31316); *tkv-CA* (BDSC36537). *yw* (BDSC189) was used for wildtype. *UAS-GFP-Mad(44)* is from Inaba lab stock.

For all crosses for obtaining *mGL-dpp* homozygous flies, one copy of *dpp* transgene (*pPA dpp 8391/X*)(*21*) was introduced to assist embryonic expression and rescue semi-lethality. For trapping HA-tagged Dpp, dppGal4 was used with Tub-Gal80ts to induce HA-trap expression for 4 days at 29°C in *HA-dpp* homozygous background.

HA-dpp, UAS-HA-trap, dppGal4, Tub-Gal80ts lines are described previously(*20*).

FasIIIGal4 was obtained from DGRC, Kyoto Stock Center (A04-1-1 DGRC#103-948).

dpp-GFP knock-in line was kind gift from Thomas Kornberg and Ryo Hattori. *UAS-histone H3-GFP* and *bamGal4* on 3rd was kind gifts from Yukiko Yamashita.

Generation of *mGL-dpp* allele

The detail procedure to generate endogenously tagged dpp alleles were previously reported(*20*). In brief, utilizing the attP sites in a MiMIC transposon inserted in the dpp locus (MiMIC dppMI03752, BDSC36399), about 4.4 kb of the dpp genomic sequences containing the second (last) coding exon of dpp including a tag and its flanking sequences was inserted in the intron between dpp's two coding exons. The endogenous exon was then removed using FLP-FRT to keep only the tagged exon. mGL (mGreenLantern(*50*)) was inserted after the last processing site to tag all the Dpp mature ligands. *mGL-dpp* homozygous flies show no obvious phenotypes. The detail characterization of these alleles will be reported elsewhere.

Generation of *UASp-bam* transgenic line

bam cDNA was PCR-amplified from cDNA pool isolated from wild-type testis (*yw*) using the following primers with restriction sites (underlined):

NotI bam Forward 5' -AC<u>GCGGCCGC</u>ACCATGCTTAATGCACGTGACGTGTGTC-3'

AscI bam Reverse 5' -AT<u>GGCGCGCC</u>TTAGCTTCTGAAGCGAGGTACACGTCCGG-3′

PCR products were then digested with NotI and AscI and ligated to a modified pPGW vector (kind gift from Michael Buszczak) using NotI and AscI sites within the multiple cloning site and verified by Sanger sequencing (Genewiz). Transgenic flies were generated using strain attP2 by PhiC31 integrase-mediated transgenesis (BestGene).

Generation of *bam* reporter transgenic lines

Bam promoter (-198 to bam 5'UTR)-Bam ORF-GFP fragments were amplified from genomic DNA isolated from bam promoter-bamGFP stock (gift from Yukiko Yamashita)[30] using combinations of following 6 primers. Overlap sequences for Gibson Assembly reaction were added for each primer.

1) SphI KpnI bam-198F: 5' -agcggatccaagcttgcatgcGGTACCccaaatcagtgtgtataatt-3′

2) GFPend-R: TAG AGG TAC CCT CGA GCC GCT TAC TTG TAC AGC TCG TCC ATG CCG -3′

3) -68mut-F: 5' -TATTTGTATTACGGCaaccctgttctggGTACTCGACATGAT-3′

4) -68mut-R: 5' -GCCGTAATACAAATAAGTTTCAATTTatggtcacc-3′

5) +39mut-F: 5' -CGCAGACAGCGTAATTTCagcgatttcaaacggtaaaaag-3′

6) +39mut-R: 5’ -GAAATTACGCTGTCTGCGaattcaggagaaagaggaagaa-3′

For wild type bam promoter, a fragment amplified by primer 1/2 was used.

For bam promoter with mutation on position -68, 1/4+2/3 fragments were used.

For bam promoter with mutation on position -39, 1/6+2/5 fragments were used.

pUAST-GFP-attB vector (gift from Cheng-Yu-Lee) was digested by SphI/NotI to remove UAS promoter located between these sites. The amplified fragments were assembled with digested vector using Gibson Assembly kit (NEB) and sequenced. Transgenic flies were generated using strain attP2 by PhiC31 integrase-mediated transgenesis (BestGene).

Induction of de-differentiation

Induction of de-differentiation was performed following previously described method with modifications(*25*). Approximately 0- to 3-day-old adult flies carrying hs-Bam (BDSC24636) transgene were raised in 22°C and heat-shocked in a 37°C water bath for 30 min twice daily in vials with fly food. Vials were placed in a 29°C incubator between heat-shock treatments. After 6-time treatments, vials were returned to 22°C for recovery. Testes were dissected at desired recovery time points.

Immunofluorescence Staining

Testes were dissected in phosphate-buffered saline (PBS) and fixed in 4% formaldehyde in PBS for 30–60 minutes. Next, testes were washed in PBST (PBS + 0.2% TritonX-100, Thermo Fisher) for at least 60 minutes, followed by incubation with primary antibody in 3% bovine serum albumin (BSA) in PBST at 4°C overnight. Samples were washed for 60 minutes (three times for 20 minutes each) in PBST, incubated with secondary antibody in 3% BSA in PBST at room temperature for 2 hours and then washed for 60 minutes (three times for 20 minutes each) in PBST. Samples were then mounted using VECTASHIELD with 4’,6-diamidino-2-phenylindole (DAPI) (Vector Lab). For pMad staining, testes were incubated with 5% BSA in PBST for 30min at room temperature prior to primary antibody incubation to reduce background. The primary antibodies used were as follows: rat anti-Vasa (1:20; developed by A. Spradling and D. Williams, obtained from Developmental Studies Hybridoma Bank (DSHB); mouse anti-Hts (1B1, 1:20; DSHB) mouse-anti-FasIII (1:20, 7G10; DSHB); mouse anti-γ-Tubulin (GTU-88;

1:400; Sigma-Aldrich); Rabbit anti-pMad (1:300; Cell Signaling); Mouse anti-phospho-Histone H3 (Ser10) Antibody, clone 3H10 (Sigma-Aldrich). AlexaFluor-conjugated secondary antibodies (Abcam) were used at a dilution of 1:400.

For Bam staining, 0.2% Tween-20 (Thermo Fisher) was used instead of TritonX-100 for PBS-T. anti-Bam (1:20) antibody was a kind gift from Michael Buszczak.

Live imaging

Testes from newly eclosed flies were dissected into Schneider's *Drosophila* medium containing 10% fetal bovine serum and glutamine–penicillin–streptomycin. These testes were placed onto Gold Seal Rite-On Micro Slides' 2 etched rings with media, then covered with coverslips. Images were taken using a Zeiss LSM800 confocal microscope with a 63× oil immersion objective (NA = 1.4) within 30 minutes. For all live imaging experiments, imaging was performed within 30 minutes.

FRAP analysis

Fluorescence recovery after photo-bleaching (FRAP) of mGL-Dpp signal was undertaken using a Zeiss LSM800 confocal laser scanning microscope with 63X/1.4 NA oil objective. Zen software was used for programming each experiment. Encircled areas of interest (randomly chosen 5µm-diameter circles from the area within less than 40 µm away from the testis tip) were photobleached using the 488 nm laser (laser power; 100%, iterations; 10). Fluorescence recovery was monitored every 10 seconds. Background signal taken in outside of the tissue in each time point were subtracted from the signal of bleached region. Dextran dye permeabilization assay was performed as described previously (*22*). Briefly, testes were incubated with 10KDa dextran conjugated to AlexaFluor-647 (Thermo Fisher, Catalog number: D22914) at a final concentration of 0.2µg/µl in 1 mL media for 10min then immediately subjected for imaging. Acquisition setting was adjusted for each sample and normalized by calculating % recovery rate.

% recovery rate was calculated as follows;

Let I^t be the intensity at each time point (t), I^{post} be the intensity at post-bleaching (first postbleach scan) and I^{pre} be the intensity at pre-bleaching. The governing equation of % recovery is: % recovery= $(I^t - I^{post})/ (I^{pre} - I^{post})$ x100.

Quantification of pMad intensities

Image-J/Fiji software was used for image quantification. Average intensity was measured for anti-pMad staining from each GSC nucleus using a single slice taken by 1AU-pinhole with 63X/1.4 NA oil objective confocal imaging, and background level measured distal region of the same testis was subtracted. Same acquisition setting was used across the samples. To normalize the staining conditions, the average intensities of pMad from four cyst cells (CCs) in the same testes were used as internal control and the ratios of intensities were calculated as each GSC per average intensities of CC. The means and s.d. were plotted to the graph for each genotype. Mean intensity values (a.u.) of CCs were unchanged for genotypes shown in Figure S1A, B (see details in main text).

Quantification of Bam staining and Bam reporter intensities

Image-J/Fiji software was used for quantification. Average intensity was measured for anti-Bam staining or GFP signal from entire region of 4 or 8 cell cysts using a single slice taken by 1AU-pinhole with 63X/1.4 NA oil objective confocal imaging, and subtracted background measured from distal area of the testis within the same slice. Same acquisition setting was used across the samples.

Scoring of centrosome and spindle orientation

Centrosome misorientation was indicated when neither of the two centrosomes were closely associated with the hub-GSC interface during interphase. Spindle misorientation was indicated when neither of the two spindle poles were closely associated with the hub-GSC interface during mitosis.

Statistical analysis and graphing

No statistical methods were used to predetermine sample size. The experiments were not randomized. The investigators were not blinded to allocation during experiments and outcome assessment. All experiments were independently repeated at least 3 times to confirm the results. Statistical analysis and graphing were performed using GraphPad Prism 9 software.

Supplemental Data Individual numerical values displayed in all graphs are provided.

Figures

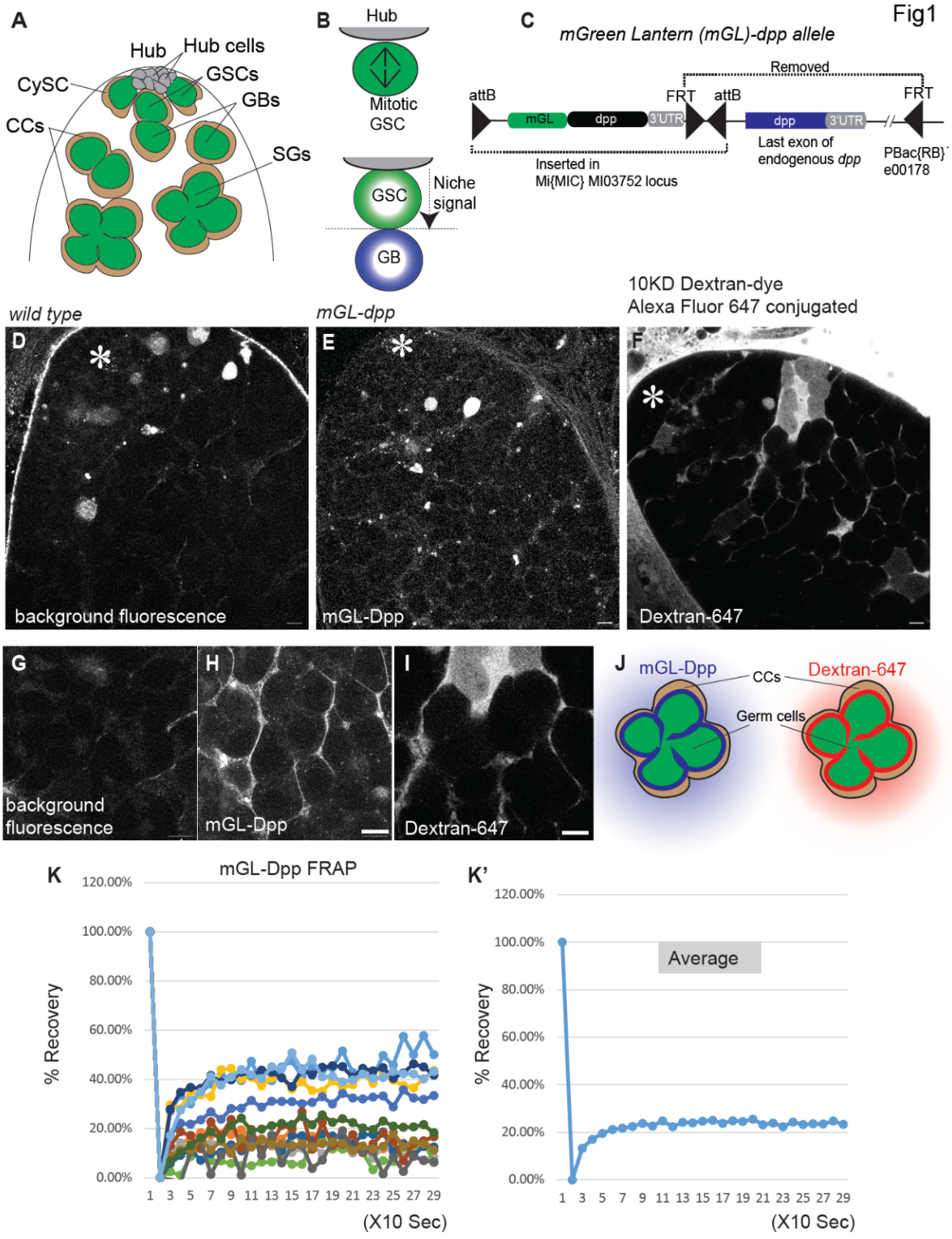

Figure 1. Dpp diffuses from niche to anterior area of testis

A) Anatomy of anterior area of Drosophila testis. Hub cells form a cluster and serve as the niche for germline stem cells (GSCs). Differentiating daughter cells or gonialblasts (GBs) undergo four rounds of incomplete division, called spermatogonia (SGs). Somatic cyst stem cells (CySCs) or cyst cells (CCs) are encapsulating developing germline. **B**) A schematic of asymmetric division (ACD) of GSCs. When the GSC divides, the mitotic spindle is always oriented perpendicularly towards hub-GSC interface (upper panel). As the result, GSC and GB are stereotypically positioned, one close to the hub and the other away from the hub (lower panel). Signal from the hub only activate juxtaposed daughter cell so that the two daughter cells can acquire distinct cell fates. **C**) A design of *mGreen Lantern (mGL)-dpp* allele. mGreen Lantern (mGL)-tagged full length dpp cording region (after last processing site) was inserted in the cassette with two attB sites and one FRT site. The cassette was inserted in MiMIC MI03752 locus, then endogenous protein cording sequence of dpp located in last exon was removed by recombination between two FRT sites (one within the cassette, the other in PBac(RB)e00178. See details in *Method*). **D, E**) Representative confocal images comparing testis tips isolated from wildtype (*yw*) and *mGL-dpp* line using the same setting for imaging. **F**) A representative confocal image of testis tips after incubated with Alexa Fluor 647 conjugated dextran-dye. Wildtype (*yw*) flies were used. **G-I**) Magnified SG areas of the testis from wildtype (*yw*, **G**) *mGL-dpp* fly (**H**) and the testis incubated with Alexa Fluor 647 dextran-dye (**I**). **J**) Anatomical interpretation of images shown in **H** and **I**., **K, K'**) Recovery curves of mGL-Dpp FRAP curves. % Recovery values (see Methods for calculation) from 14 trials are shown in **K**. Values from each trial are shown in different colors. **K'** shows average values of 14 trials.

All scale bars represent 10 μm. Asterisks indicate approximate location of the hub. In all images and graphs, live tissues were used.

Fig2

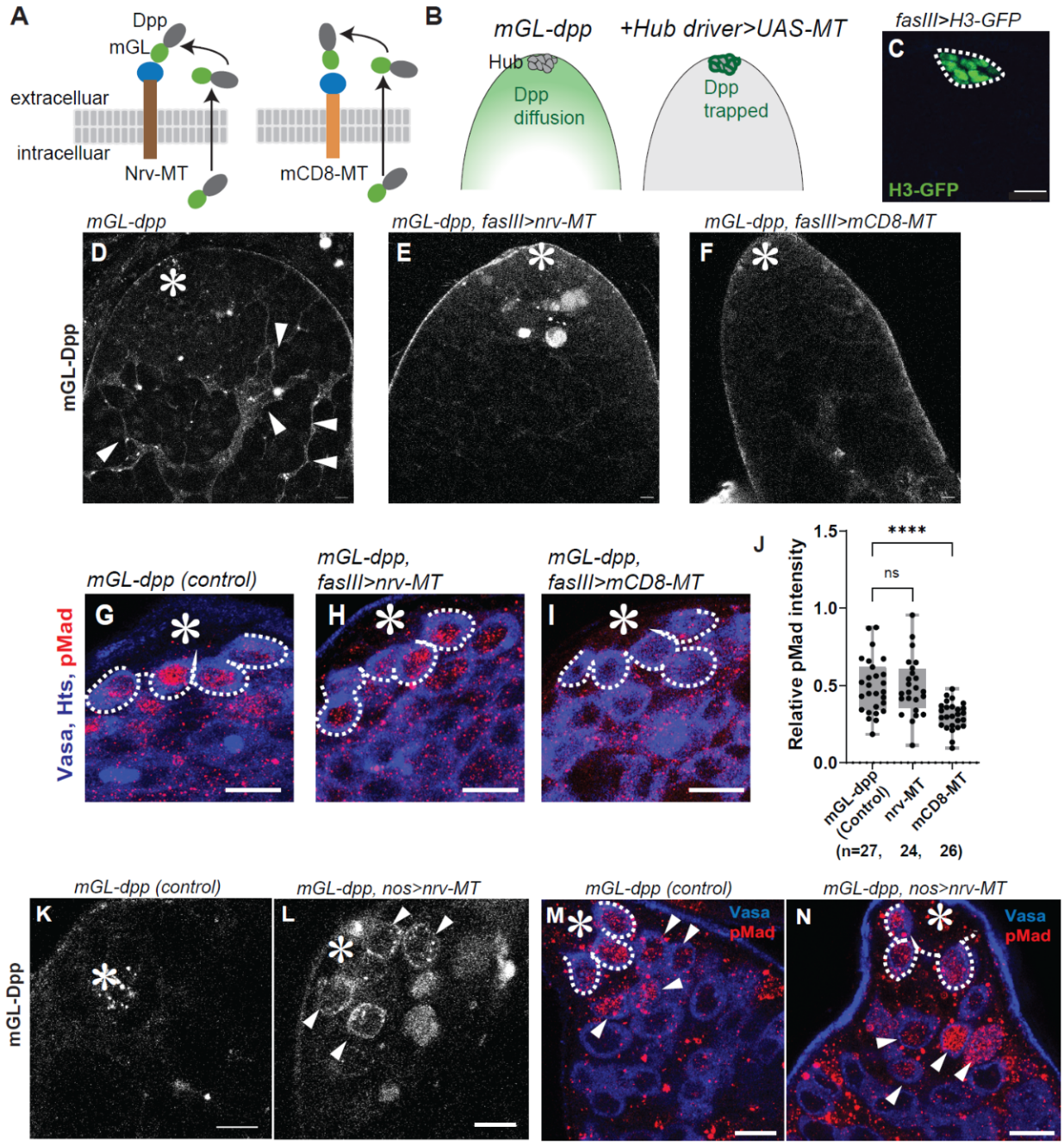

Figure 2. Perturbation of Dpp diffusion without affecting niche-GSC signal

A) Schematics of the design to trap Dpp on the surface of Dpp producing cells using Morphotrap (MT), the genetically encoded synthetic receptor for GFP-tagged proteins. The nanobody, vhhGFP4 (blue circle), that specifically binds to GFP, is fused to extracellular domain of either mouse CD8 transmembrane protein (mCD8-MT) or Nrv1 basolateral protein scaffold (Nrv-MT). **B**) Expected outcome of hub-driven expression of morphotrap in the background of *mGL-dpp* homozygous testis. Diffusing fraction of Dpp (left panel) will be trapped on the hub cell surface and no diffusing Dpp will be observed (right panel). **C**) Representative images of Histone H3-GFP expressed under the hub-specific driver, fasIIIGal4. **D-F**) Representative images of *mGL-dpp* testis tip without (**D**) or with fasIIIGal4 driven Nrv-MT expression (**E**) or with fasIIIGal4 driven mCD8-MT expression (**F**). Arrowheads in **D** show mGL-Dpp signal along the surface of SG cysts. Such signal was completely disappeared in Morphotrap expressing samples (**E** and **F**). **G-I**) Representative images of pMad staining of GSCs after trapping Dpp using indicated Morphotrap lines. The fasIIIGal4 driver was used. White broken lines encircle GSCs. **J**) Quantification of pMad intensity in GSCs (relative to CCs) of fasIIIGal4 driven Nrv-MT or mCD8-MT expressing testes in *mGL-dpp* homozygous background. P-values were calculated by Dunnett's multiple comparisons test and provided as ** $P < 0.001$ or ns; non-significant ($P \geq 0.05$). "n" indicates the number of scored GSCs. Data are means and standard deviations.

K, L) Representative images of live testis tip of *mGL-dpp* fly without (**K**) or with (**L**) expressing Nrv-MT under the germline specific driver, nosGal4. Trapped mGL-Dpp signal is seen on the surface of early germ cells in **L** (white arrowheads). **M, N**) pMad staining shows emerging pMad positive germ cells outside of the niche in *mGL-dpp, nos>nrv-MT* testis (arrowheads in **N**). pMad positive germ cells are normally only seen in GSCs and immediate descendants around the hub (arrowheads in **M**). White broken lines encircle GSCs.

All scale bars represent 10 μm. Asterisks indicate approximate location of the hub. Live tissues were used for **C-F, K, L** and fixed samples were used for **G-I, M, N**.

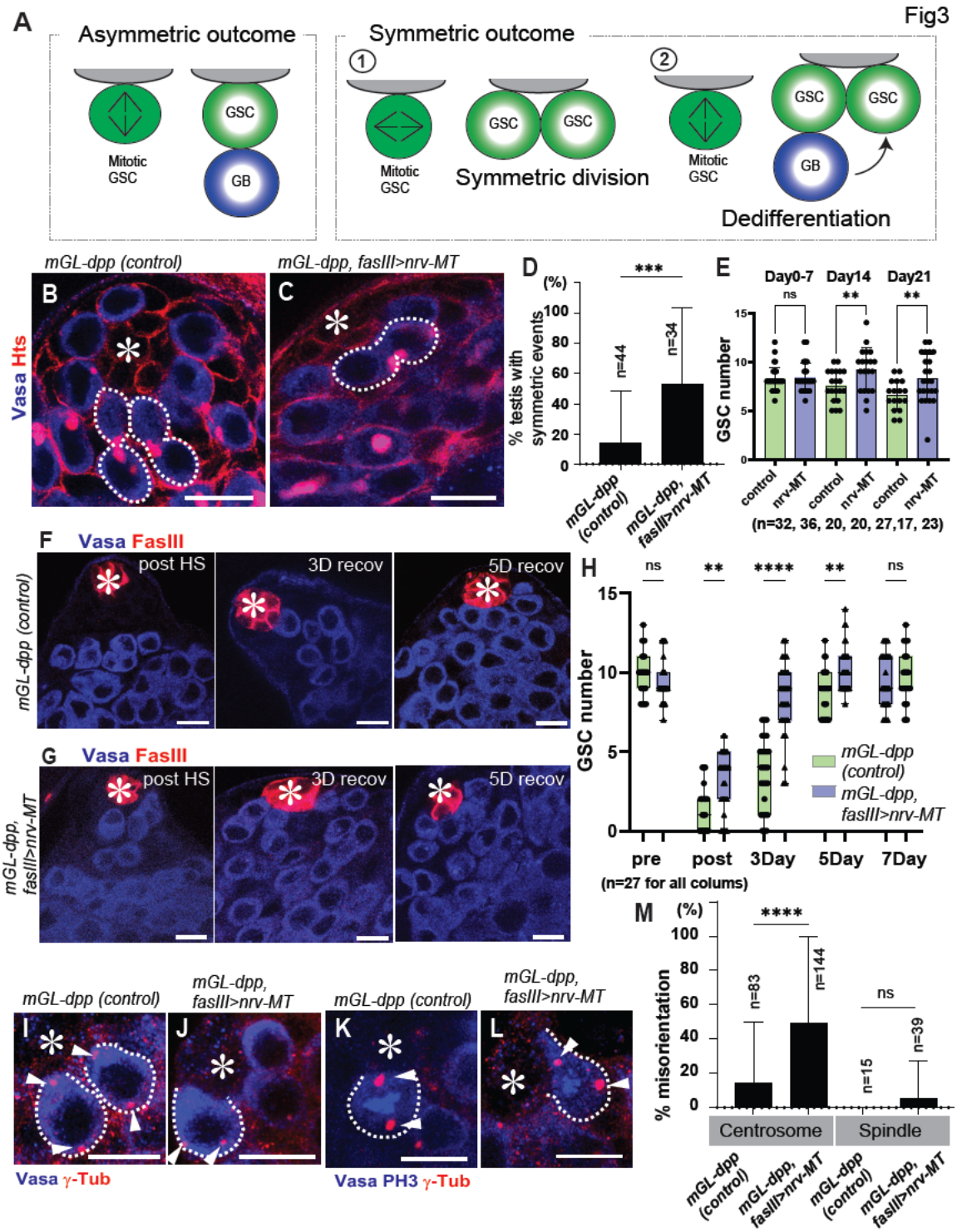

Figure 3. Diffusing fraction of Dpp prevents de-differentiation

A) Asymmetric and symmetric outcomes of GSC division. Symmetric outcome is defined as the case in which two daughter cells of a GSC division are both placed near the hub, resulting in production of two GSCs. It occurs as the consequence of either "symmetric division" (1) or "de-differentiation" (2) (see details in main text). **B, C**) Representative images of testis tip without (**B**) or with (**C**) trapping Dpp. Broken lines indicate asymmetric events in **B** and a symmetric event in **C**. **D**) Frequency of testes showing any symmetric events without or with trapping Dpp. The p-value was calculated by student-t-test *** $P < 0.0001$. **E**) Changes in GSC number during aging without or with trapping Dpp. P-values were calculated by Šídák's multiple comparisons test and provided as ** $P < 0.001$ or ns; non-significant ($P \geq 0.05$). **F, G**) Representative images of testis tip after depletion of GSC by expressing Bam (post HS; after 6-time heat shock treatment) and after 3-day recovery (3D recov) in room temperature culture without (**F**) or with (**G**) trapping Dpp. Broken lines indicate the edges of front most germ cells. **H**) Changes in GSC number during recovery from forced differentiation of GSCs without or with trapping Dpp. P-values were calculated by Šídák's multiple comparisons test and provided as ** $P < 0.001$, **** $P < 0.00001$ or ns; non-significant ($P \geq 0.05$). **I-L**) Representative images of centrosomes (**I, J**) and spindles (**K, L**) of GSCs without (**I, K**) or with (**J, L**) trapping Dpp. **M**) Percentages of misoriented centrosome and spindle in GSCs without or with trapping Dpp. P-values were calculated by Šídák's multiple comparisons test and provided as **** $P < 0.00001$ or ns; non-significant ($P \geq 0.05$).

For trapping Dpp in this figure, Nrv-MT was expressed under the control of fasIIIGal4 driver in *mGL-dpp* homozygous background. m*GL-dpp* homozygous flies without Nrv-MT expression were used for control. Fixed samples were used for all images and graphs.

All scale bars represent 10 μm. Asterisks indicate approximate location of the hub.

"n" indicates the number of scored testes in **D**, **E** and **H**, or scored GSCs in **M**. Data are means and standard deviations.

Fig4

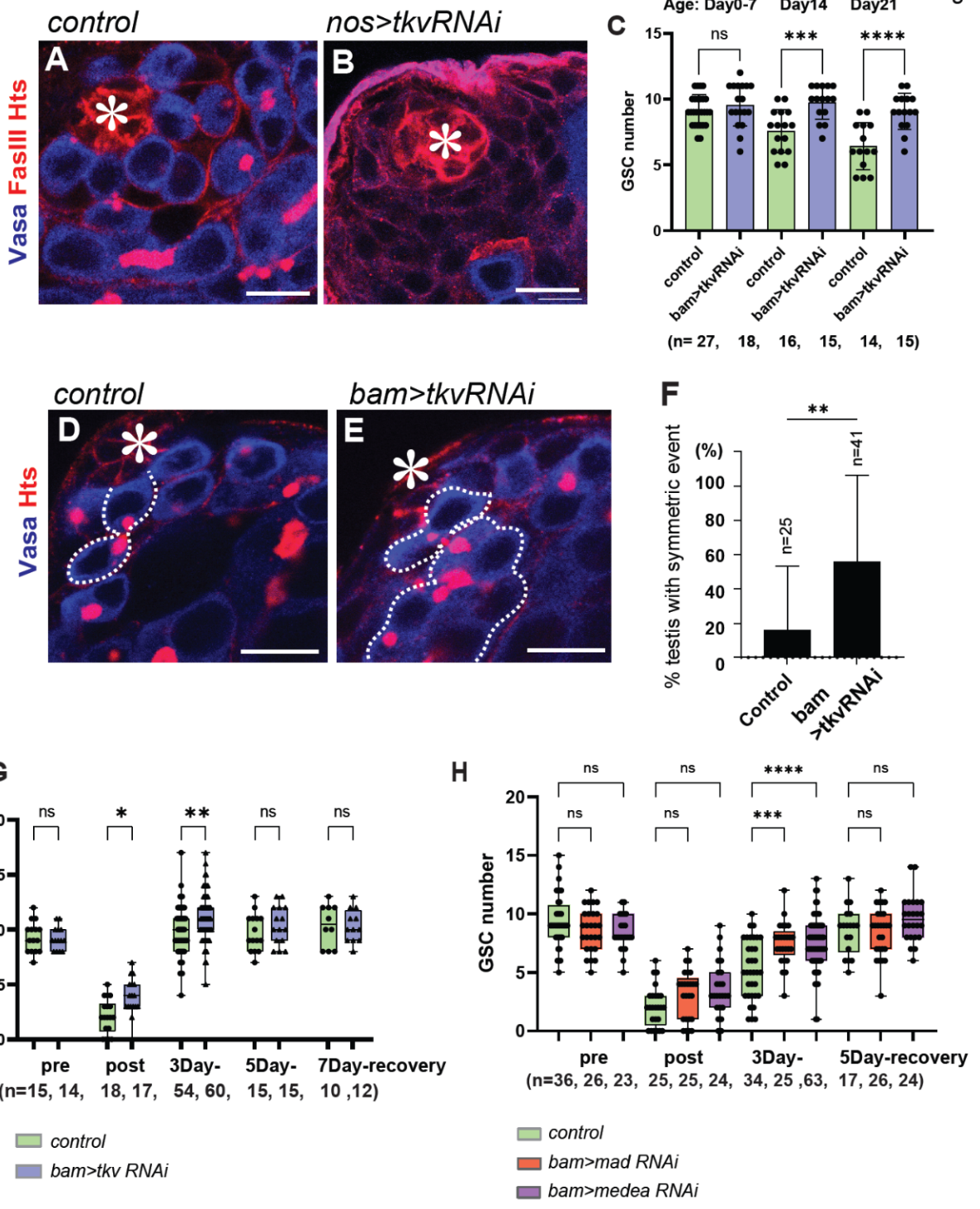

Figure 4. Dpp acts through its canonical pathway both in GSC and in differentiating germ cells

A, B) Representative images of testis tip without (**A**) or with (**B**) shRNA expression against Tkv (Tkv RNAi) under the nosGal4 driver. **C**) Changes in GSC number during aging without or with Tkv RNAi expression under the bamGal4 driver. P-values were calculated by Šídák's multiple comparisons test and provided as *** $P < 0.0001$ **** $P < 0.00001$ or ns; non-significant ($P \geq 0.05$). **D, E**) Representative images of testis tip without (**D**) or with (**E**) Tkv RNAi expression under the bamGal4 driver. Broken lines indicate symmetric events. **F**) Frequency of testes showing any symmetric events without or with bam>Tkv RNAi. The p-value was calculated by student-t-test ** $P < 0.001$. **G, H**) Changes in GSC number during recovery from forced differentiation of GSCs without or with bam>Tkv RNAi (**G**), Mad RNAi, Medea RNAi (**H**). P-values were calculated by Šídák's multiple comparisons test and provided as **** $P < 0.00001$, ***$P < 0.0001$ or ns; non-significant ($P \geq 0.05$).

All scale bars represent 10 μm. Asterisks indicate approximate location of the hub. Fixed samples were used for all images and graphs. Fixed samples were used for scoring. “n” indicates the number of scored testes in **C**, **F**, **G** and **H**. Data are means and standard deviations.

Fig5

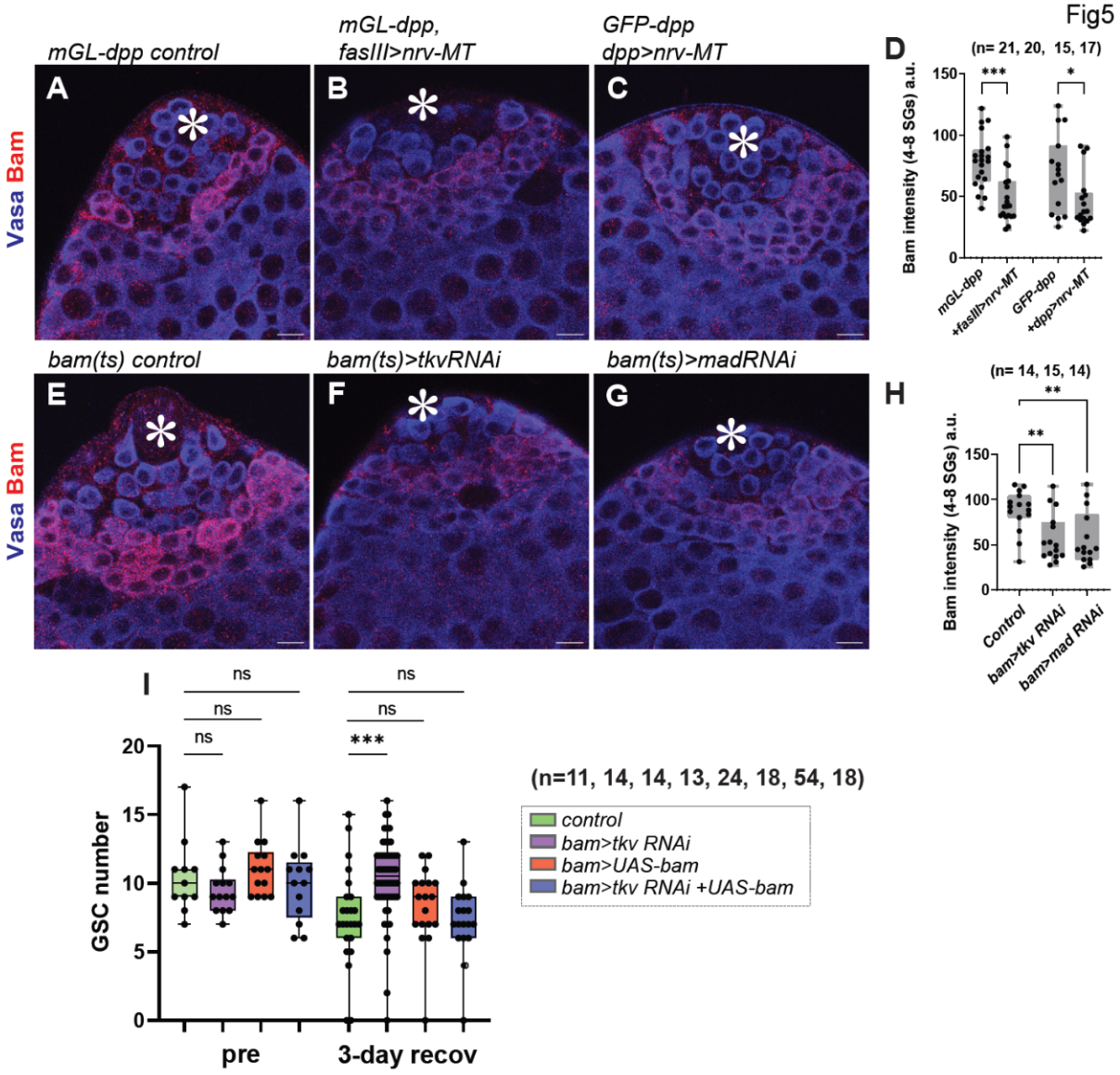

Figure 5. Dpp signal oppositely regulates Bam expression in GSCs and in differentiating germ cells

A-C) Representative images of Bam staining after prevention of Dpp diffusion. Two combinations of driver and background genotype was used as indicated. **D**) Quantification of Bam intensity in 4-8 cell SGs of indicated genotypes. P-values were calculated by Šídák's multiple comparisons test and provided as **** $P < 0.00001$. **E-G)** Representative images of Bam staining of indicated RNAi experiments. BamGal4 (no VP16) driver was used with TubGal80ts and crossed with each RNAi line at room temperature, then progenies were dissected after 3-day temperature shift at 29°C. BamGal4, TubGal80ts without RNAi was used for the control. **H**) Quantification of Bam intensity in 4-8 cell SGs of indicated genotypes shown in **E-G**. P-values were calculated by Dunnett's multiple comparisons test and provided as **** $P < 0.00001$. **I**) Changes in GSC number during recovery from forced differentiation of GSCs in indicated genotypes. P-values were calculated by Šídák's multiple comparisons test and provided as * $P < 0.05$, ** $P < 0.001$ or ns; non-significant ($P \geq 0.05$).

All scale bars represent 10 μm. Asterisks indicate approximate location of the hub. Fixed samples were used for all images and graphs.

Fixed samples were used for scoring. “n” indicates the number of scored testes in **D**, **H** and **I**. Data are means and standard deviations.

Fig6

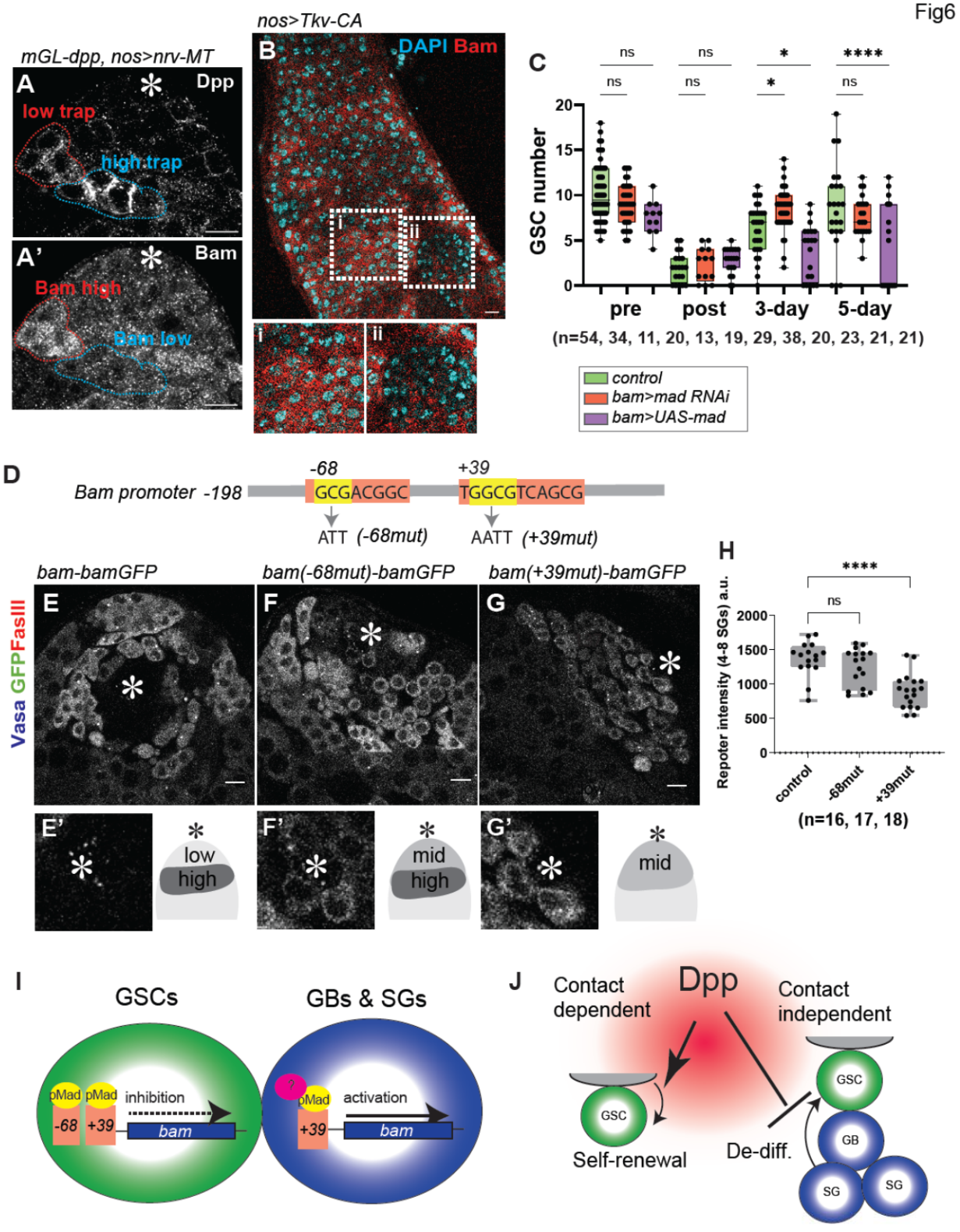

Figure 6. Two pMad binding sites in *bam* promoter contribute to opposed signaling outcomes

A, A') Representative images of Bam staining of the testis trapping Dpp on germ cell membrane (mGL-Dpp, nos>Nrv-MT). mGL-Dpp channel is shown in **A**, Bam staining channel is shown in **A'**. Encircled areas show 4-8 SGs with low-level Dpp trap (red), high-level Dpp trap (blue). **B)** A representative image of the tumor with Bam staining in the testis of flies expressing Tkv-CA under the nosGal4 driver. Lower panels are magnification of squared regions, i and ii in the upper panel. **C**) Changes in GSC number during recovery from forced differentiation of GSCs without or with overexpression of Mad (UAS-Mad), knockdown of Mad (Mad RNAi) under the bamGal4 driver P-values were calculated by Šídák's multiple comparisons test and provided as **** $P < 0.00001$, *$P < 0.01$ or ns; non-significant ($P \geq 0.05$). **D**) Structure of *bam* promoter region containing two Mad binding sites. Mad binding sequences are shown for both sites. Core sequences are shown in yellow boxes and were mutated for mutant reporter constructs as shown in below (GCG to ATT, GGCG to AATT, respectively). **E-G)** Representative images of GFP signal in the testis of flies harboring indicated Bam reporters. Live testes were used for GFP quantification. Graphical interpretation of each image is shown below. **E'-G')** Magnified niche area containing hub and GSCs. For detection of the hub location, electronically switchable illumination and detection module (ESID) was used. **H**) Quantification of reporter intensity in 4-8 cell SGs of indicated reporters. P-values were calculated by Dunnett's multiple comparisons test and provided as **** $P < 0.00001$ or ns; non-significant ($P \geq 0.05$).

I) Model. High concentration of pMad occupy two Mad binding sites in GSCs, which is required for full suppression of bam expression. Low concentration of pMad binds to +39 Mad binding domain which is required for upregulation of bam in GB and SGs. Binding of a co-activator (pink circle) may be required for full activation of bam. **J**) Model. Dpp ligand has effect on GSCs contact dependent manner and on differentiating germ cells (GBs and SGs) through diffusion from the hub. Dpp is required for stem cell maintenance (Self-renewal), whereas its diffusing fraction promotes differentiation of daughter cells via preventing de-differentiation (De-diff).

All scale bars represent 10 μm. Asterisks indicate approximate location of the hub. Fixed samples were used for all images and graphs.

Fixed samples were used for **A-C**. Live tissues were used for **E-H**. In **C** and **H**, "n" indicates the number of scored testes. Data are means and standard deviations.

References

1. R. Schofield, The relationship between the spleen colony-forming cell and the haemopoietic stem cell. *Blood Cells* **4**, 7-25 (1978).
2. D. T. Scadden, Nice neighborhood: emerging concepts of the stem cell niche. *Cell* **157**, 41-50 (2014).
3. T. A. Rando, Stem cells, ageing and the quest for immortality. *Nature* **441**, 1080-1086 (2006).
4. S. J. Morrison, J. Kimble, Asymmetric and symmetric stem-cell divisions in development and cancer. *Nature* **441**, 1068-1074 (2006).
5. M. Inaba, Y. M. Yamashita, M. Buszczak, Keeping stem cells under control: New insights into the mechanisms that limit niche-stem cell signaling within the reproductive system. *Molecular Reproduction and Development* **83**, 675-683 (2016).
6. D. A. Dansereau, P. Lasko, The development of germline stem cells in Drosophila. *Methods Mol Biol* **450**, 3-26 (2008).
7. Y. M. Yamashita, D. L. Jones, M. T. Fuller, Orientation of asymmetric stem cell division by the APC tumor suppressor and centrosome. *Science* **301**, 1547-1550 (2003).
8. M. de Cuevas, E. L. Matunis, The stem cell niche: lessons from the Drosophila testis. *Development* **138**, 2861-2869 (2011).
9. J. Zhang, L. Li, BMP signaling and stem cell regulation. *Developmental Biology* **284**, 1-11 (2005).
10. A. A. Shivdasani, P. W. Ingham, Regulation of Stem Cell Maintenance and Transit Amplifying Cell Proliferation by TGF-β Signaling in Drosophila Spermatogenesis. *Current Biology* **13**, 2065-2072 (2003).
11. E. Kawase, M. D. Wong, B. C. Ding, T. Xie, Gbb/Bmp signaling is essential for maintaining germline stem cells and for repressing bam transcription in the Drosophilatestis. *Development* **131**, 1365-1375 (2004).
12. J. L. Leatherman, S. Dinardo, Germline self-renewal requires cyst stem cells and stat regulates niche adhesion in Drosophila testes. *Nat Cell Biol* **12**, 806-811 (2010).
13. C. Schulz *et al.*, A misexpression screen reveals effects of bag-of-marbles and TGF beta class signaling on the Drosophila male germ-line stem cell lineage. *Genetics* **167**, 707-723 (2004).
14. N. Tulina, E. Matunis, Control of stem cell self-renewal in Drosophila spermatogenesis by JAK-STAT signaling. *Science* **294**, 2546-2549 (2001).
15. M. Inaba, M. Buszczak, Y. M. Yamashita, Nanotubes mediate niche-stem-cell signalling in the Drosophila testis. *Nature* **523**, 329-332 (2015).
16. M. Inaba, S. M. Ridwan, M. Antel, Removal of cellular protrusions. *Seminars in Cell & Developmental Biology* **129**, 126-134 (2022).
17. S. Ladyzhets *et al.*, Self-limiting stem-cell niche signaling through degradation of a stem-cell receptor. *PLOS Biology* **18**, e3001003 (2020).
18. S. Harmansa, F. Hamaratoglu, M. Affolter, E. Caussinus, Dpp spreading is required for medial but not for lateral wing disc growth. *Nature* **527**, 317-322 (2015).
19. S. Harmansa, I. Alborelli, D. Bieli, E. Caussinus, M. Affolter, A nanobody-based toolset to investigate the role of protein localization and dispersal in Drosophila. *eLife* **6**, e22549 (2017).
20. S. Matsuda *et al.*, Asymmetric requirement of Dpp/BMP morphogen dispersal in the Drosophila wing disc. *Nat Commun* **12**, 6435 (2021).

21. F. M. Hoffmann, W. Goodman, Identification in transgenic animals of the Drosophila decapentaplegic sequences required for embryonic dorsal pattern formation. *Genes Dev* **1**, 615-625 (1987).
22. M. J. Fairchild, F. Islam, G. Tanentzapf, Identification of genetic networks that act in the somatic cells of the testis to mediate the developmental program of spermatogenesis. *PLOS Genetics* **13**, e1007026 (2017).
23. V. Salzmann, M. Inaba, J. Cheng, Y. M. Yamashita, Lineage tracing quantification reveals symmetric stem cell division in Drosophila male germline stem cells. *Cell Mol Bioeng* **6**, 441-448 (2013).
24. X. R. Sheng, E. Matunis, Live imaging of the Drosophila spermatogonial stem cell niche reveals novel mechanisms regulating germline stem cell output. *Development* **138**, 3367-3376 (2011).
25. X. R. Sheng, C. M. Brawley, E. L. Matunis, Dedifferentiating Spermatogonia Outcompete Somatic Stem Cells for Niche Occupancy in the Drosophila Testis. *Cell Stem Cell* **5**, 191-203 (2009).
26. S. C. Herrera, E. A. Bach, JNK signaling triggers spermatogonial dedifferentiation during chronic stress to maintain the germline stem cell pool in the Drosophila testis. *eLife* **7**, e36095 (2018).
27. S. Schwitalla *et al.*, Intestinal Tumorigenesis Initiated by Dedifferentiation and Acquisition of Stem-Cell-like Properties. *Cell* **152**, 25-38 (2013).
28. C. Brawley, E. Matunis, Regeneration of Male Germline Stem Cells by Spermatogonial Dedifferentiation in Vivo. *Science* **304**, 1331-1334 (2004).
29. J. Cheng *et al.*, Centrosome misorientation reduces stem cell division during ageing. *Nature* **456**, 599-604 (2008).
30. T. Bollenbach *et al.*, Precision of the Dpp gradient. *Development* **135**, 1137-1146 (2008).
31. D. Chen, D. M. McKearin, A discrete transcriptional silencer in the bam gene determines asymmetric division of the Drosophila germline stem cell. *Development* **130**, 1159-1170 (2003).
32. D. Chen, D. McKearin, Dpp Signaling Silences bam Transcription Directly to Establish Asymmetric Divisions of Germline Stem Cells. *Current Biology* **13**, 1786-1791 (2003).
33. Z. Guo, Z. Wang, The glypican Dally is required in the niche for the maintenance of germline stem cells and short-range BMP signaling in the Drosophila ovary. *Development* **136**, 3627-3635 (2009).
34. M. Liu, T. M. Lim, Y. Cai, The Drosophila female germline stem cell lineage acts to spatially restrict DPP function within the niche. *Sci Signal* **3**, ra57 (2010).
35. R. E. Harris, M. Pargett, C. Sutcliffe, D. Umulis, H. L. Ashe, Brat promotes stem cell differentiation via control of a bistable switch that restricts BMP signaling. *Dev Cell* **20**, 72-83 (2011).
36. V. Van De Bor *et al.*, Companion Blood Cells Control Ovarian Stem Cell Niche Microenvironment and Homeostasis. *Cell Rep* **13**, 546-560 (2015).
37. X. Wang, R. E. Harris, L. J. Bayston, H. L. Ashe, Type IV collagens regulate BMP signalling in Drosophila. *Nature* **455**, 72-77 (2008).
38. L. Xia *et al.*, The niche-dependent feedback loop generates a BMP activity gradient to determine the germline stem cell fate. *Curr Biol* **22**, 515-521 (2012).
39. S. Eliazer *et al.*, Lsd1 restricts the number of germline stem cells by regulating multiple targets in escort cells. *PLoS Genet* **10**, e1004200 (2014).
40. C. Y. Tseng *et al.*, Smad-Independent BMP Signaling in Somatic Cells Limits the Size of the Germline Stem Cell Pool. *Stem Cell Reports* **11**, 811-827 (2018).
41. X. Jiang *et al.*, Otefin, a nuclear membrane protein, determines the fate of germline stem cells in Drosophila via interaction with Smad complexes. *Dev Cell* **14**, 494-506 (2008).
42. L. Xia *et al.*, The Fused/Smurf complex controls the fate of Drosophila germline stem cells by generating a gradient BMP response. *Cell* **143**, 978-990 (2010).

43. C. Schulz, C. G. Wood, D. L. Jones, S. I. Tazuke, M. T. Fuller, Signaling from germ cells mediated by the rhomboid homolog stet organizes encapsulation by somatic support cells. *Development* **129**, 4523-4534 (2002).
44. J. Sardi *et al.*, Mad dephosphorylation at the nuclear pore is essential for asymmetric stem cell division. *Proceedings of the National Academy of Sciences* **118**, e2006786118 (2021).
45. M. O. Casanueva, E. L. Ferguson, Germline stem cell number in the Drosophila ovary is regulated by redundant mechanisms that control Dpp signaling. *Development* **131**, 1881-1890 (2004).
46. D. Nellen, R. Burke, G. Struhl, K. Basler, Direct and Long-Range Action of a DPP Morphogen Gradient. *Cell* **85**, 357-368 (1996).
47. C. S. Hill, Transcriptional Control by the SMADs. *Cold Spring Harb Perspect Biol* **8**, (2016).
48. G. A. Challen, N. C. Boles, S. M. Chambers, M. A. Goodell, Distinct hematopoietic stem cell subtypes are differentially regulated by TGF-beta1. *Cell Stem Cell* **6**, 265-278 (2010).
49. S. M. Park *et al.*, Musashi-2 controls cell fate, lineage bias, and TGF-β signaling in HSCs. *J Exp Med* **211**, 71-87 (2014).
50. B. C. Campbell *et al.*, mGreenLantern: a bright monomeric fluorescent protein with rapid expression and cell filling properties for neuronal imaging. *Proceedings of the National Academy of Sciences* **117**, 30710-30721 (2020).